Computational Materials Science 118 (2016) 147–154

Contents lists available at ScienceDirect

Computational Materials Science

journal homepage: www.elsevier.com/locate/commatsci

Diversity of monomeric dioxo chromium species in Cr/silicalite-2 catalysts: A hybrid density functional study

Mehdi Ghambarian [a], Zahra Azizi [b], Mohammad Ghashghaee [c,*]

[a] Gas Conversion Department, Faculty of Petrochemicals, Iran Polymer and Petrochemical Institute, P.O. Box 14975-112, Tehran, Iran
[b] Department of Chemistry, Karaj Branch, Islamic Azad University, P.O. Box 31485-313, Karaj, Iran
[c] Faculty of Petrochemicals, Iran Polymer and Petrochemical Institute, P.O. Box 14975-112, Tehran, Iran

ARTICLE INFO

Article history:
Received 8 September 2015
Received in revised form 15 February 2016
Accepted 4 March 2016
Available online 25 March 2016

Keywords:
Chromium
Silicalite-2
ZSM-11 zeolite
DFT
Gibbs free energy
Cluster modeling

ABSTRACT

The present paper deals with the theoretical characterization of the dioxo Cr species exchanged into the silicalite-2 structure via hybrid density functional theory with cluster models to represent the active site. The molecular models range from a simple mono silicon atom ring to more complex Cr–siloxane rings of 7T atoms. The common B3LYP and M06 density functionals were used for the calculations. The results indicate that the chemical hardness increases from a complex ring to a simple geminate type. Overall, the QTAIM calculations point to intermediate ionic–covalent nature of the Cr–oxygen bonds. An excellent correlation is found between the positive eigenvalue of the Hessian at the bond critical point with the Cr—O bond distance. Whereas the enthalpy change on the exchange reaction alters from −20.3 to 56.1 kcal/mol at the M06/6-311+G* level, the binding energy lies in a shorter range of 907.5–926.6 kcal/mol. As concluded from the Gibbs free energy changes on the exchange reaction with both of the methods, only the clusters of 4T size or larger would be formed spontaneously. However, M06 predicts ∼13% stronger bindings for the Cr ion. Overall, the electronic properties depend upon both the Si—O—Cr—O—Si aperture size and the local configuration of the matrix. Furthermore, a fivefold coordination of Cr is accompanied with a lower ionization potential, a longer Cr—O distance, and a less negative charge on the terminal O atoms.

1. Introduction

The well-known CrO_x/SiO_2 Phillips catalyst has been estimated to produce over one-third of high-density polyethylene (HDPE) [1], amounting to ∼12 million tons of annual HDPE production worldwide [2]. Chromium oxide catalysts are also employed commercially for production of light olefins from alkanes. Although the alumina support has been used in most of industrial dehydrogenation technologies [3–6], CrO_x catalysts on different silica materials have attracted much interest in the open literature for dehydrogenation of ethane [7–9], propane [10], and isobutene [11], oxidative dehydrogenation of ethane in the presence of carbon dioxide [9,12–15], oxidative dehydrogenation of propane with oxygen [16], conversion of styrene to benzaldehyde [17], liquid-phase oxidation of cyclohexane [18], oxidation of primary amines to corresponding nitro compounds [19], epoxidation of alkenes [20], acetylene cyclotrimerization [21], and oxidation of phenol with hydrogen peroxide [22].

Although much interest and research have been expended into Cr/SiO_2 systems experimentally for the last five decades [23], only a few serious relevant theoretical studies have appeared quite recently. Therefore, the structures of the surface Cr species in different environments are still to be determined unambiguously, and computational chemistry can provide us with complementary data not accessible through experiments [24]. A number of theoretical works [23–29], e.g., have addressed monomeric Cr(VI) species on silica. In addition, $Cr(II)O_x/SiO_2$ Phillips catalysts have been modeled theoretically [21,30,31]. Redox chromia Cr(III) sites on silica have also been investigated as the main/original active sites in alkane dehydrogenation [32–34].

The framework of ZSM-11 (MEL type) and its all-silica variant silicalite-2 consists of pentasil layers joined in such a way that the adjacent layers are enantiomeric and are stacked by a

---

Abbreviations: BCP, bond critical point; DFT, density functional theory; FMO, frontier molecular orbital; HDPE, high-density polyethylene; HOMO, highest occupied molecular orbital; LUMO, lowest unoccupied molecular orbital; NBO, natural bond orbital; NNN, next-nearest-neighbor; QTAIM, quantum theory of atoms in molecules.

* Corresponding author. Tel.: +98 21 48662481; fax: +98 21 44787032.
E-mail address: m.ghashghaee@ippi.ac.ir (M. Ghashghaee).

http://dx.doi.org/10.1016/j.commatsci.2016.03.009

σ-reflection. The framework atoms shape a two-dimensional network of straight pores with perpendicular intersections. If the neighboring pentasil layers are adjoined instead by an inversion, but again enantiomerically, an MFI-type (ZSM-5 or silicalite-1) structure is obtained [35–37]. Thus, silicalite-2 has a three-dimensional pore structure composed of straight channels of about 5.30–5.40 Å with a free diameter of about 8.90 Å at the intersections [38].

As an effective silica-based transition metal catalyst, Cr/silicalite-2 has also been the subject of interest in several experimental works [13,15,19,20,22,39–42]. However, the silicalite-2 structure has been employed as a catalyst support for metals other than Cr as well [43]. To the best of our knowledge, however, no theoretical study has been reported that explores different structures of Cr within an ordered silicalite framework. In this contribution, the plausible structures and properties of monomeric Cr(VI) oxide species on the silicalite-2 surface under dehydrated conditions are then investigated theoretically with the viable cluster models of the Cr/silicalite-2 system.

2. Computational method

The cluster modeling approach was employed for the simulations. Fig. 1 shows the unit cell of silicalite-2 structure. A careful slicing and exploring within a unit cell provided all types of the defect sites available in silicalite-2. As a common practice [44,45], all of the dangling bonds were saturated by H atoms fixed along the direction of the bond with the next oxygen or silicon eliminated from the cluster model in compliance with the crystallographic data [46]. The Cr ion with the immediate neighbors including the O atoms from two defect hydroxyl groups were allowed to relax during the geometry optimizations. As also confirmed earlier [47], the rest of the silicalite cluster was kept frozen to abide by the mechanical restrictions of the solid matrix.

The structural optimizations were performed using hybrid functionals B3LYP [48–50] and M06 [51] along with the standard 6-31+G* basis set [52–55], which are known to be reliable on both oxides and metal clusters [45,56–58]. Improved energetic results were also obtained through single-point calculations at a higher level with a 6-311+G* basis set [59] based on the B3LYP/6-31+G* and M06/6-31+G* geometries. The natural bond orbital (NBO) population [60] and the QTAIM [61–66] analyses on the optimized structures were carried out at the B3LYP/6-311+G* level.

The ion exchange or stabilization energies (ΔE_{ex}) for the cluster models were estimated according to the following reaction [23]:

$$[\mathrm{SiO}]\text{—}(\mathrm{OH})_2 + \mathrm{H_2CrO_4} \rightarrow [\mathrm{SiO}]\text{—}\mathrm{O_2CrO_2} + 2\mathrm{H_2O} \qquad (1)$$

The binding energies (ΔE_{b}) of Cr ions at the defect sites of silicalite-2 were also calculated for the reaction given below:

$$[\mathrm{SiO}]\text{—}\mathrm{O_2CrO_2} \rightarrow [\mathrm{SiO}]\text{—}\mathrm{O_2^{2-}} + \mathrm{CrO_2^{2+}} \qquad (2)$$

The calculations were implemented using NWChem 6.5 [67] and Multiwfn 3.3.8 [68]. Finally, the graphical outputs were drawn by the molecular visualization program Mercury 3.3 [69–72].

3. Results and discussion

As a reasonable approach to commence, the available defect sites of a silicate-2 material for attachment of dioxo chromium species would be classified in terms of the interatomic length between the next-nearest-neighbor (NNN) Si atoms to the Cr ion. Table 1 shows such a classification for silicalite-2 based on the crystallographic data. As can be seen in this table, different oxide rings can be present ranging from a simple 2T mono silicon atom (T refers to the Si and Cr atoms) to di, tri, tetra, penta, and hexa ones, with an estimate of their individual varieties according to the SiO—Cr—OSi (or shortly TCrT) aperture size. No TCrT aperture length is reported for the first model, which is obtained from the interaction of a dioxo Cr ion with two geminal OH groups (HO—Si—OH) on the same silicon atom.

Fig. 2 displays the optimized geometries of all of the obtained cluster models. The B1–B5 series of models relate to those dioxo Cr species chemisorbed on two vicinal silanol groups located at the two ends of a siloxane bridge (HO—Si—O—Si—OH). Differently from the rest of the series, the Cr ion in B4 and B5 is in close proximity to both Si and O atoms of the siloxane group. The remaining models in Table 1 represent more complex interactions of the dioxo Cr ion with adjacent nonvicinal Si—OH groups (not directly connected) at two defect sites of the surface linked by two or more consecutive siloxane bridges (Fig. 2). In general, the TCrT aperture distance varied from 3.03 to 5.15 Å for B1 to D4 clusters, respectively. No stable sites were found for the dioxo digrafted chromates at larger TCrT aperture lengths. Moreover, no higher-membered rings were taken into account as every position for accommodation of the dioxo species in such larger rings were found to reduce to one of a smaller size already considered. For the coming comparisons of the different cluster models, as also adopted earlier [24], it will be assumed that the distribution of dioxo Cr species at the defect sites of silicalite-2 is controlled by their thermodynamic stability and not by the kinetics of the preparation method.

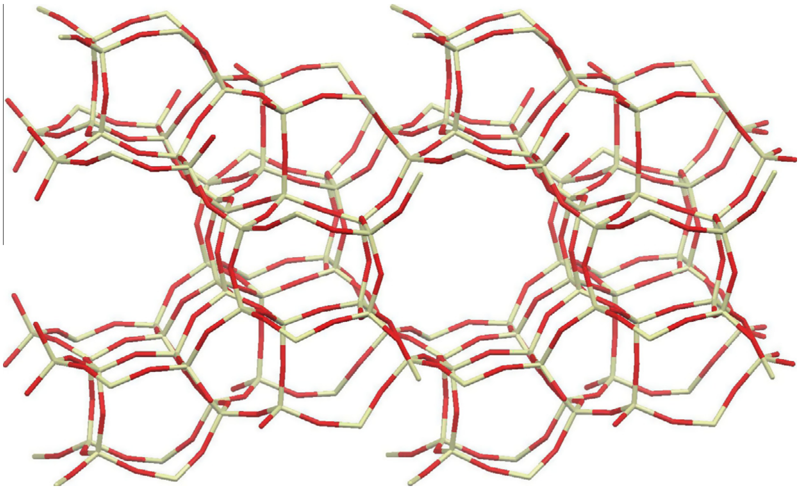

Fig. 1. The silicalite-2 matrix viewed at the (010) layer.